



Since January 2020 Elsevier has created a COVID-19 resource centre with free information in English and Mandarin on the novel coronavirus COVID-19. The COVID-19 resource centre is hosted on Elsevier Connect, the company's public news and information website.

Elsevier hereby grants permission to make all its COVID-19-related research that is available on the COVID-19 resource centre - including this research content - immediately available in PubMed Central and other publicly funded repositories, such as the WHO COVID database with rights for unrestricted research re-use and analyses in any form or by any means with acknowledgement of the original source. These permissions are granted for free by Elsevier for as long as the COVID-19 resource centre remains active.



Subunit microparticulate vaccine delivery using microneedles trigger significant SARS-spike-specific humoral and cellular responses in a preclinical murine model

Smital Patil, Sharon Vijayanand, Devyani Joshi, Ipshita Menon, Keegan Braz Gomes, Akanksha Kale, Priyal Bagwe, Shadi Yacoub, Mohammad N. Uddin, Martin J. D'Souza*

Center for Drug Delivery Research, Vaccine Nanotechnology Laboratory, College of Pharmacy, Mercer University, Atlanta, GA 30341, USA

ARTICLE INFO

Keywords:

Subunit vaccine
Spike glycoprotein
Microparticles
Microneedles
Antibody levels
Cellular response
Coronavirus

ABSTRACT

The objective of this “proof-of-concept” study was to evaluate the synergistic effect of a subunit microparticulate vaccine and microneedles (MN) assisted vaccine delivery system against a human coronavirus. Here, we formulated PLGA polymeric microparticles (MPs) encapsulating spike glycoprotein (GP) of SARS-CoV as the model antigen. Similarly, we formulated adjuvant MPs encapsulating Alhydrogel® and AddaVax™. The antigen/adjuvant MPs were characterized and tested *in vitro* for immunogenicity. We found that the antigen/adjuvant MPs were non-cytotoxic *in vitro*. The spike GP MPs + Alhydrogel® MPs + AddaVax™ MPs showed enhanced immunogenicity *in vitro* as confirmed through the release of nitrite, autophagy, and antigen presenting molecules with their co-stimulatory molecules. Next, we tested the *in vivo* efficacy of the spike GP MP vaccine with and without adjuvant MPs in mice vaccinated using MN. The spike GP MPs + Alhydrogel® MPs + AddaVax™ MPs induced heightened spike GP-specific IgG, IgG1 and IgG2a antibodies in mice. Also, spike GP MPs + Alhydrogel® MPs + AddaVax™ MPs enhanced expression of CD4+ and CD8+ T cells in secondary lymphoid organ like spleen. These results indicated spike GP-specific humoral immunity and cellular immunity *in vivo*. Thus, we employed the benefits of both the subunit vaccine MPs and dissolving MN to form a non-invasive and effective vaccination strategy against human coronaviruses.

1. Introduction

Over the past two decades, the world has experienced two epidemics and a pandemic due to the emergence of coronaviruses affecting humans, beginning with the novel Severe Acute Respiratory Syndrome Coronavirus (SARS-CoV) that emerged in 2002, with a mortality rate of 10 % in the general population and 50 % in the older population (Ma et al., 2020). Later, Middle East Respiratory Syndrome Coronavirus (MERS-CoV) appeared in 2012, with a severe fatality rate of 35 % (MERS-CoV). In 2019 novel SARS-CoV-2 surfaced, with a mortality rate ranging from 0.1 to 2 % (Ritchie et al., 2020). Among the three human coronaviruses, SARS-CoV and MERS-CoV had higher mortality rates than SARS-CoV-2. These viruses cause severe respiratory syndrome, pneumonia, bronchiolitis, sinusitis, and other systemic symptoms (Smith et al., 2020). These viruses belong to the *coronaviridae* family and consist of four structural proteins: spike protein (S), nucleocapsid protein (N), membrane protein (M), and envelope protein (E). The S protein

is a transmembrane homotrimer class I fusion glycoprotein consisting of two functional subunits: S1 and S2 (Du et al., 2009).

Furthermore, the S1 subunit comprises the receptor binding domain (RBD), critical in the virus binding to the human angiotensin-converting enzyme-2 (ACE-2) receptor, especially alveolar epithelial cells, thus mediating the entry of these viruses in the host cells. Both SARS-CoV and SARS-CoV-2 utilize the ACE-2 receptor in the host for entry (Giordano et al., 2021). SARS-CoV and SARS-CoV-2 share genetic similarities of about 61 % in the S1 subunit and 90 % in the S2 subunit (Hatmal et al., 2020). Due to the similarities in both these viruses, we sought to utilize the spike glycoprotein (GP) of the SARS-CoV virus as a model antigen to evaluate our vaccination strategy against coronaviruses.

Delivery of vaccine antigen by polymeric microparticles (MPs) has been extensively studied and employed in vaccine design (Joshi et al., 2021; Menon et al., 2021; Gala et al., 2018). Soluble antigens such as recombinant proteins are known to be relatively less immunogenic due to their short half-life, mainly activating MHC-II pathway and

* Corresponding author at: 3001 Mercer University Dr, DV-108, Atlanta, GA 30341, USA.

E-mail address: dsouza_mj@mercer.edu (M.J. D'Souza).

<https://doi.org/10.1016/j.ijpharm.2023.122583>

Received 12 August 2022; Received in revised form 29 December 2022; Accepted 2 January 2023

Available online 4 January 2023

0378-5173/© 2023 Elsevier B.V. All rights reserved.

demonstrating poor cross-presentation of soluble antigen (Storni et al., 2005; Silva et al., 2016; Allahyari and Mohit, 2015). Instead, encapsulating the soluble antigen in a biodegradable polymeric matrix has exhibited protection of antigen and increased cellular uptake by antigen-presenting cells (APCs) due to the increased size and effective cross-presentation of exogenous antigens by MHC-I pathway, which is essential to invade viral infections by presenting the antigen to CD8+ cytotoxic T cells (Silva et al., 2016). It has been reported that particles with sizes ranging from 0.1 to 3 μm are better targeted by APCs, particularly dendritic cells, which further aid in inducing helper and cytotoxic T-cell responses (Storni et al., 2005; Carcaboso et al., 2004; Rice-Ficht et al., 2010). Especially, polymers such as poly(lactic-co-glycolic acid) PLGA offer multiple advantages when used to formulate particulate delivery systems, such as excellent biodegradability, and biocompatibility, thus decreasing cytotoxicity (Nano-Microparticle). The double emulsion solvent evaporation method has been developed and studied to prepare vaccine nano/microparticles (Bilati et al., 2005). The double emulsion method is preferred for recombinant protein vaccines as through the single emulsification method; the proteins can easily diffuse in the aqueous phase causing low entrapment of hydrophilic agents such as proteins or peptides (Allahyari and Mohit, 2015). Hence, to preserve the biological activity of the recombinant protein, we utilized the double emulsion solvent evaporation technique. Here, we formulated MPs encapsulating the spike GP in PLGA polymer and studied the immunogenicity of this vaccine candidate.

The incorporation of immunomodulatory agents such as adjuvants further aids in enhancing vaccine-induced immunity by activation of APCs (Pulendran et al., 2021). Formulation of adjuvants into MPs is advantageous for the following reasons: 1) polarization of the immune response towards Th1 or Th2 response, 2) minimizing side effects of the adjuvant distributed systemically (O'Hagan and Singh, 2003). Alhydrogel®, a licensed and widely-used vaccine adjuvant, enhances uptake by APCs and induces Th2 immune responses by activating CD4+ helper T cells (Alhydrogel; InvivoGen). Alhydrogel® stimulates a longer immune response owing to the repository effect, which promotes the interaction of antigen with APCs by maintaining the antigen's physical and chemical properties (He Peng et al., 2015). One of the major challenges during vaccine development with Alhydrogel® is attributed to the restricted range of immune responses (Brewer, 2006). Additionally, AddaVax™, a squalene-based oil-in-water nano-emulsion, acts by recruiting and activating APCs and has been shown to induce both Th1 and Th2 immune responses by activating CD4+ helper T cells and CD 8+ cytotoxic T cells (AddaVax™; InvivoGen). Thus, we evaluated spike GP MPs' *in vitro* and *in vivo* immunogenicity with both the adjuvants Alhydrogel® and AddaVax™ in microparticulate form.

Most current vaccines against COVID-19 employ the traditional and more invasive intramuscular route of administration (Munro et al., 2022). Therefore, exploring non-invasive routes of vaccination, such as intradermal vaccine delivery with dissolving microneedles (MN), will be beneficial for developing a more compliant vaccine capable of producing a robust immune. Due to the high abundance of dendritic cells in the skin and its efficient drainage to lymph nodes, skin is known to be an attractive site for vaccination. The skin is known to be an organ armed with immune surveillance consisting of major APCs such as Langerhans cells (LCs) and dermal dendritic cells (Joshi et al., 2021; Streilein, 1983; Sparber et al., 2010). Moreover, MN is minimally invasive as they do not reach the dermal layer, which holds nerve endings (Menon et al., 2021; Prausnitz et al., 2009; Leone et al., 2017). MN vaccine approach further offers multiple advantages, such as the potential for the vaccine to be self-administered, thereby lessening the burden of immunization on healthcare providers as well as being minimally invasive. Self-administration is one of the major advantages which can lead to rapid mass vaccination globally, especially during a pandemic (Menon et al., 2021; Prausnitz et al., 2009). Thus, to evaluate this route for vaccine delivery, we fabricated quick-dissolving microparticulate vaccine-loaded MN and tested its immunogenic potential *in vivo* in a

preclinical murine model.

Although formulation and *in vitro* immunogenicity of vaccines as polymeric nano/microparticles have been studied for multiple infectious diseases (Nano-Microparticle; O'Hagan and Singh, 2003), delivery of a subunit microparticulate vaccine using MN against a human coronavirus has not yet been studied. Thus, the objective of this proof-of-concept study was to formulate a model subunit vaccine-polymeric MPs encapsulating the spike GP to evaluate its *in vitro* immunogenicity with adjuvant MPs and assess the induction of humoral and cellular immune responses *in vivo* when delivered using dissolving MN. Thus, here we demonstrate that the synergistic effects of a subunit vaccine loaded in polymeric MPs and delivered using dissolving MN can prove to be a powerful immunization tool against diseases caused by coronaviruses.

2. Materials and methods

2.1. Materials

The antigen, spike GP, was obtained from BEI Resources, NIAID (National Institute of Allergy and Infectious Diseases), NIH (National Institutes of Health): SARS-CoV Spike (S) Protein delta™, Recombinant from Baculovirus, NR-722. Sodium Hyaluronate (MW 100 kDa) was purchased from Lifecore biomedical (Chaska, MN, USA). Poly(lactic-co-glycolic) acid (PLGA) 75:25 (Resomer® RG 752H) of MW 4000–15000 Da was purchased from Evonik Industries, (Alabama). Dichloromethane (DCM) was purchased from Fischer Scientific. Span® 80 and trehalose dihydrate were obtained from Millipore Sigma (Burlington, MA, USA). 3-(4,5-Dimethylthiazol-2-yl)-2,5-diphenyltetrazolium bromide (MTT) and Pierce Micro BCA Assay Kit was purchased from ThermoFischer (Waltham, MA). The 8*8 array polydimethylsiloxane (PDMS) MN molds were obtained from Micro point Technologies (Singapore). Murine dendritic cells (DC 2.4) were kindly provided by Dr. Kenneth L. Rock (Dana-Farber Cancer Institute Inc., Boston, MA, USA). CYTO-ID® Autophagy detection kit was obtained from Enzo Life Sciences (Farmingdale, NY, USA). Anti-mouse antibodies conjugated with fluorescent markers such as allophycocyanin-labeled for MHC I (clone AF6-88.5.5.3), MHC II (clone M5/114.15.2), CD4 (clone GK1.5) and fluorescein isothiocyanate-labeled CD86 (clone GL1), CD40 (clone 3/23), CD8a (clone 53–6.7) were obtained from eBioscience laboratories (San Diego, CA, USA) and BioLegend (San Diego, CA, USA). Adjuvants such as Alhydrogel® (alum) and AddaVax™ (MF59-like adjuvant) were obtained from InvivoGen (San Diego, CA, USA). Horseradish peroxidase (HRP)-conjugated goat anti-mouse secondary IgM, IgG, IgG1, and IgG2a antibodies were purchased from Invitrogen (Rockford, IL, USA). 3,3',5,5'-tetramethylbenzidine (TMB) was purchased from Becton, Dickinson & Co. (Franklin Lakes, New Jersey, USA). 6–8 weeks-old Swiss Webster mice were purchased from Charles River Laboratories (Wilmington, MA, USA). Cell culture supplies such as Dulbecco's Modified Eagle's Medium (DMEM), trypsin EDTA solution, fetal bovine serum (FBS), and penicillin/streptomycin (pen-strep) were purchased from American Type Culture Collection (Manassas, VA, USA).

2.2. Methods

2.2.1. Formulation of spike GP and adjuvant PLGA MPs

SARS-CoV Spike GP-loaded PLGA MPs were formulated using a double emulsion solvent evaporation technique developed previously in our laboratory (Braz Gomes et al., 2022). Briefly, PLGA was dissolved in DCM to obtain a 2 % w/v polymer solution to form the organic phase. Next, a 0.05 % w/v spike GP antigen in PBS solution, with 0.03 % v/v Span 80 as the primary emulsifier, was added to the polymer solution and homogenized using an Omni THQ probe homogenizer at 17000 rpm to form the primary water-in-oil emulsion. The primary emulsion was then added to 0.1 % PVA solution and homogenized to form the water-in-oil-in-water double emulsion. The final emulsion was kept under

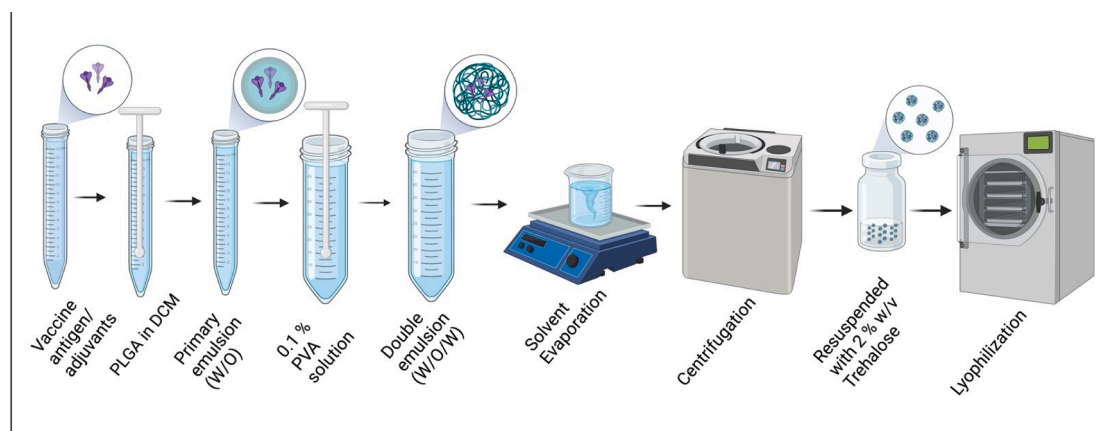


Fig. 1. Formulation process of PLGA MPs with Spike Glycoprotein.

constant stirring for 5 h to facilitate solvent evaporation of DCM and hardening of the particles. The emulsion was then centrifuged at 15,000 rpm for 15 min at 4 °C to obtain the MPs. The MPs were then resuspended in deionized water containing 2 % w/v trehalose as a cryoprotectant and lyophilized using a Labconco™ benchtop freeze dryer to obtain a freeze-dried powder. MPs of Adjuvants were formulated separately, each using Alhydrogel® and AddaVax™ as adjuvants. The adjuvant MPs were formulated using the double emulsion solvent evaporation method described above, followed by lyophilization. Fig. 1 is a schematic representation of the formulation process for MPs.

2.2.2. Characterization of spike GP and adjuvants loaded MPs

The formulated MPs were characterized for particle size, polydispersity index (PDI), and zeta potential using Zetasizer Nano ZS (Malvern Pananalytical). Briefly, 2 mg MPs were suspended in 1000 µL of deionized water and transferred to a polystyrene cuvette and disposable folded capillary cells to measure particle size/polydispersity index (PDI) and zeta potential, respectively. The particle size and PDI was analyzed by dynamic light scattering, and zeta potential was analyzed by electrophoretic light scattering using a Zetasizer Nano ZS (Malvern Pananalytical). The particle size, PDI, and zeta potential were also measured for blank and adjuvant-loaded MPs. The formulated MPs were next visualized for shape and morphology using scanning electron microscopy (SEM). The MPs were suspended in deionized water and mounted on the stubs with double-sided carbon tabs of 12 mm. The MPs were then allowed to dry to remove residual moisture. The MPs were then observed using the scanning electron microscope, Phenom™ benchtop SEM, Nanoscience Instruments, Phoenix, AZ. The different batches of the formulated MPs were averaged for average percent recovery yield. The following formula was used to calculate the percent recovery yield of MPs after lyophilization:

$$\text{Percent recovery yield (\%)} = \frac{\text{Weight of MPs post-lyophilization}}{\text{Weight of solid ingredients in the formulation pre-lyophilization}} \times 100$$

2.2.3. Assessment of protein content in spike GP MP

The encapsulation efficiency of the formulated particles was evaluated using a Pierce™ BCA (Bicinchoninic acid) assay kit. Briefly, the 2 mg of Spike GP MPs were suspended in 1 mL of DCM to dissolve PLGA. Further, these samples were centrifuged at 3000 rpm for 10 min, and the residual DCM was allowed to evaporate in a fume hood; the residue was then dissolved in 0.01 M PBS. BCA assay was performed according to the manufacturer's instructions to analyze the antigen content. Spike GP was then quantified using the standard curve plotted using Pierce™ BCA assay kit to obtain the concentration per mL of the protein. For the calculation of percent encapsulation efficiency following formula was used:

$$\text{Encapsulation Efficiency} = \frac{\text{Experimental protein content in MPs}}{\text{Theoretical protein content in MPs}} \times 100$$

2.2.4. Quantification of nitrite release using Griess's assay

The innate immune response can be characterized by the release of nitric oxide (NO) and its metabolites like nitrite, which was quantified using Griess's assay. Murine dendritic cells (DC 2.4) were grown using DMEM with 10 % FBS and 5 % pen-strep in a T-75 flask. After 80 % confluency, the cells were plated in a 48-well plate at a seeding density of 3×10^4 cells/well. Next, the following groups were tested: no treatment (cells only), spike GP suspension, blank MPs, spike GP MPs, spike GP MPs with Alhydrogel® MPs, and spike GP MPs with Alhydrogel® MPs and AddaVax™ MPs (MPs equivalent to 5 µg of Spike GP antigen for vaccine MPs, 5 µg of Alhydrogel® and 1 µg of AddaVax™ for adjuvant MPs) for 48 h at 37 °C and 5 % CO₂. Next, 100 µL of the cell supernatant was transferred to another 48-well plate, and freshly prepared 1 % sulfanilamide in 5 % o-phosphoric acid and 0.1 % N-(1-naphthylethylenediamine) solutions were added in equal quantities which resulted in conversion of nitrite released by cells and later formation of pink-red azo dye compound. The plate absorbance was read at 540 nm using a Bio-Tek Synergy H1 microplate reader (BIO-TEK Instruments, Winooski, VT). The nitrite concentration was quantified using a standard curve for sodium nitrite (1 mM stock concentration of sodium nitrite).

2.2.5. Determination of cytotoxicity of MPs

The formulated antigen and adjuvant MPs were evaluated for cytotoxicity towards DC 2.4 using an MTT assay. Briefly, DC 2.4 were plated in a 96-well plate at a seeding density of 10^4 cells/well and incubated overnight at 37 °C and 5 % CO₂. MPs in a range from 5 µg/mL to 500 µg/mL were incubated with the cells for 24 h at 37 °C and 5 % CO₂. A cells only group was the negative control group, and cells exposed to dimethylsulfoxide (DMSO) served as the positive control group. After incubation, the supernatant was discarded after which 20 µL of 0.22 µm filtered MTT reagent (5 mg/1 mL PBS) was added to each well. The plate was incubated at 37 °C for 3 h, protected from light. Next, DMSO was added to the wells to dissolve the purple formazan crystals and the plate was kept on a shaker for 15 min at room temperature, protected from light. The absorbance was measured at 570 nm.

2.2.6. Evaluation of expression of autophagosomes in DC 2.4

The expression of autophagosomes in DC 2.4 was assessed with fluorescence microscopy and flow cytometry using a CYTO-ID® autophagy detection kit. Briefly, DC 2.4 were plated in a 24-well plate at a seeding density of 5×10^4 cells per well and allowed to incubate overnight at 37 °C and 5 % CO₂. The cells were treated with the following groups: untreated (cells only), spike GP suspension, blank MPs, Spike GP MPs, Spike GP MPs + Alhydrogel® MPs, and Spike GP MPs + Alhydrogel® MPs + AddaVax™ MPs (MPs equivalent to 5 µg of Spike GP antigen for vaccine MPs, 5 µg of Alhydrogel® and 1 µg of

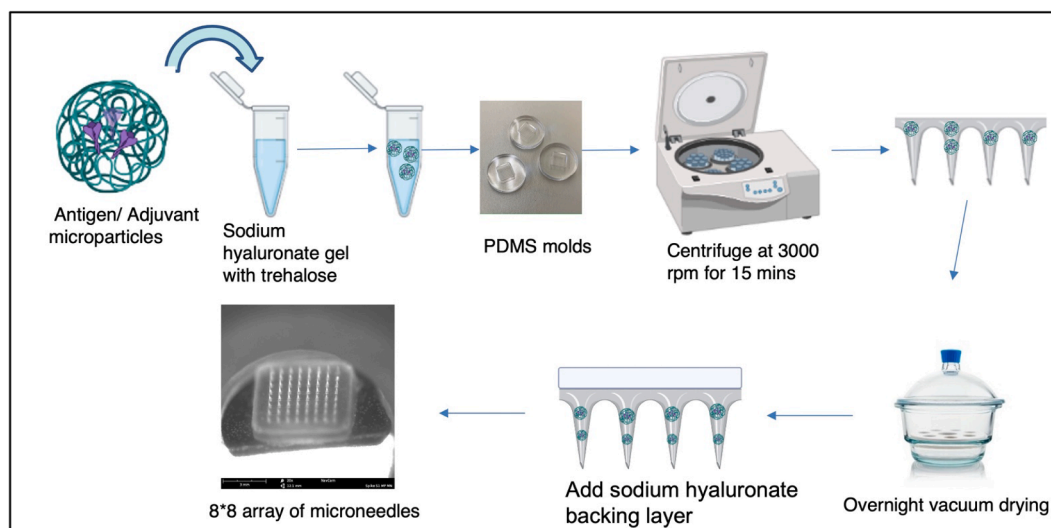


Fig. 2. Formulation process of polymeric dissolving microneedles loaded with microparticulate vaccine.

AddaVax™ for adjuvant MPs) for 24 h and incubated at 37 °C and 5 % CO₂. For fluorescence microscopy, cells were washed with PBS and stained with CYTO-ID® dye and Hoechst 33342 Nuclear stain for 30 min at 37 °C. After the incubation period, the unbound dye was washed, and the cells were observed under DAPI and FITC filters of a fluorescence microscope (Lionheart FX, Biotek, VT, USA). In a DC 2.4, the cell nucleus was stained with Hoechst 33342 Nuclear stain and observed as blue color, and autophagosomes were stained with CYTO-ID® dye and observed as green color. Quantitative expression of autophagosomes in DC 2.4 was determined by the same method as above, except that the cells were only stained with the CYTO-ID® dye. Next, the cells were gently trypsinized and analyzed for the percent of cells expressing autophagosomes using flow cytometry (BD Accuri C6 Plus flow cytometer; BD Bioscience, San Jose, CA).

2.2.7. Quantification of expression of antigen presenting molecules and their co-stimulatory molecules in antigen presenting cells

We studied the expression of antigen-presenting molecules and their co-stimulatory molecules in DC 2.4. Briefly, DC 2.4 were plated in a 48-well plate at a seeding density of 3×10^4 cells/well. Expression of antigen-presenting molecules and their co-stimulatory molecules was evaluated in the following groups: no treatment (cells only), spike GP suspension, blank MPs, Spike GP MPs, Spike GP MPs + Alhydrogel® MPs and Spike GP MPs + Alhydrogel® MPs + AddaVax™ MPs (MPs equivalent to 5 µg of Spike GP antigen for vaccine MPs, 5 µg of Alhydrogel® and 1 µg of AddaVax™ for adjuvant MPs). Cells were exposed to treatments for 48 h at 37 °C with 5 % CO₂. The cells were trypsinized and incubated with allophycocyanin-labeled and fluorescein isothiocyanate-labeled anti-mouse with the following pairs MHC-I, CD86 and MHC-II, CD40 according to manufacturer's instructions (eBioscience laboratories, San Diego, CA), respectively for 1 h at 4 °C. Excess marker was washed with PBS before fluorescence intensity was measured using a BD Accuri C6 Plus flow cytometer (BD Bioscience, San Jose, CA) (Joshi et al., 2021).

2.2.8. Formulation and characterization of dissolving MN vaccine

Dissolving MN were prepared using a method previously developed in our laboratory using the spin casting method (Braz Gomes et al., 2022). Briefly, spike GP MPs with Alhydrogel® MPs and AddaVax™ MPs were suspended in 5 % w/v of trehalose solution. Further, sodium hyaluronate was added to the suspension to form a hydrogel. 25 mg of hydrogel was added to the PDMS molds, which were then centrifuged at 3000 rpm for 15 mins at 15 °C. The MN were allowed to dry overnight in a vacuum desiccator after which a concentrated sodium hyaluronate

Table 1

Vaccination Study groups description and the vaccine dose received *in vivo*.

Vaccine Group (n = 4)	Description of vaccine received	Route of Vaccination	Dose of antigen and adjuvant MPs in MNs per subject
Naïve Blank MPs MN	– PLGA MPs without antigen or adjuvants in MNs	– Intradermal	– MPs equivalent to 20 µg of vaccine antigen
Spike GP Suspension MN	Spike GP suspension only in MNs	Intradermal	Spike GP- 20 µg
Spike GP MPs MN	Spike GP PLGA MPs in MNs	Intradermal	MPs equivalent to: Spike GP- 20 µg
(Spike GP MPs + Alhydrogel® MPs) MN	Spike GP PLGA MPs and Alhydrogel® PLGA MPs in MNs	Intradermal	MPs equivalent to: (Spike GP- 20 µg Alhydrogel® – 20 µg)
(Spike GP MPs + Alhydrogel® MPs + Addavax™ MPs) MN	Spike GP PLGA MPs, Alhydrogel® PLGA MPs and Addavax™ PLGA MPs in MNs	Intradermal	MPs equivalent to: (Spike GP – 20 µg Alhydrogel® – 30 µg Addavax™- 5 µL)

solution backing layer was added. The MN were dried overnight, removed from the PDMS molds using double-sided tape, and placed on 3 M tape to provide a band-aid-like supportive base. The formulated MN were characterized for shape, needle length and morphology using SEM. The formulated MN were also visualized after application on the murine skin under SEM. Fig. 2 represents a schematic of the formulation process of dissolving MN.

2.2.9. In vivo vaccination with antigen and adjuvant loaded MPs in MN

Six-eight-week-old Swiss Webster (CFW) mice obtained from Charles River Laboratories, Wilmington, MA, were used for testing the efficacy of the microparticulate-loaded MN vaccine. The studies were carried out as per the approved Mercer University IACUC protocol. The mice were randomly assigned into the treatment groups (n = 4), as shown in Table 1. All the groups received treatment as mentioned in Table 1. Briefly, one day prior to immunization, mice hair on the dorsal region was removed using depilatory cream. The mice were vaccinated intradermally with one prime dose and two booster doses at weeks 0, 3 and 5 respectively.

2.2.10. Detection of serum antibody levels in mice sera

Serum samples were collected bi-weekly before each dose at weeks 2,

Table 2

Characterization of microparticles for recovery yield, particle size, polydispersity index, and zeta potential.

Characterization Parameters	Spike GP MPs	Alhydrogel® MPs	AddaVax™ MPs
Recovery yield (in %)	88.03 ± 0.72	90.55 ± 0.77	89.81 ± 0.77
Particle Size (in nm)	1155.20 ± 666.95	1192.10 ± 688.25	1053.06 ± 607.98
Polydispersity index	0.55 ± 0.32	0.64 ± 0.37	0.67 ± 0.38
Zeta Potential (in mV)	-25.1 ± 1.01	-20.26 ± 0.88	-25.77 ± 0.85

4, 6 and 8. In brief, serum was isolated and analyzed for spike GP-specific IgM, IgG, IgG1, and IgG2a titers using enzyme-linked immunosorbent assay (ELISA). First, high-binding 96-well plates (Microton®) were coated with Spike GP (500 ng/well) and kept overnight at 4 °C. The plates were blocked with 3 % bovine serum albumin (BSA) for 3 h at 37 °C. Serum samples diluted in 1 % w/v BSA to 1:50 were added to the wells and incubated overnight at 4 °C. The following day, horseradish peroxidase-conjugated secondary goat anti-mouse IgM, IgG, IgG1, or IgG2a antibodies were added to the wells (1:2000–1:5000) and incubated at 37 °C for 1.5 h. Next, 50 µL of TMB substrate was added to each well. The reaction was stopped by adding 50 µL of 0.1 M H₂SO₄. Before every step, the plates were washed thrice with 0.05 % w/v PBS-Tween solution. The plate was read at 450 nm (Leleux and Roy, 2013).

2.2.11. Detection of spike GP specific T cell responses in spleen

At week 12, mice were sacrificed, and their spleen samples were harvested. Spleen samples were passed through a 40 µm cell strainer to obtain a single-cell suspension. The cells were centrifuged at 1200 rpm for 8 mins. The supernatant was discarded, and the cells were treated with ammonium chloride potassium (ACK) lysis buffer for 3 min to allow lysis of red blood cells (RBCs). This process was repeated twice to obtain a single-cell suspension of splenocytes. The cells were then centrifuged and resuspended in DMEM containing 70 % FBS, 5 % DMSO and stored at -80 °C for further analysis of T cell expression. CD4+ and CD8+ T cells in splenocytes were determined in the following manner. The cells were thawed on ice and suspended in complete DMEM. The cells were plated on a 24-well plate at 5 × 10⁴ seeding density and were stimulated with 5 µg of spike GP suspension for 24 h. Cells were then washed with PBS and incubated for 1 h to be stained with APC-labeled CD4 and FITC-labeled CD8 anti-mouse antibodies. The cells were washed 3 times with PBS and analyzed using flow cytometry.

2.2.12. Statistical analysis

GraphPad Prism version 9.2.0 for Windows (GraphPad Software, San Diego, CA) was used to conduct all statistical analyses. Comparisons

Release of nitrite

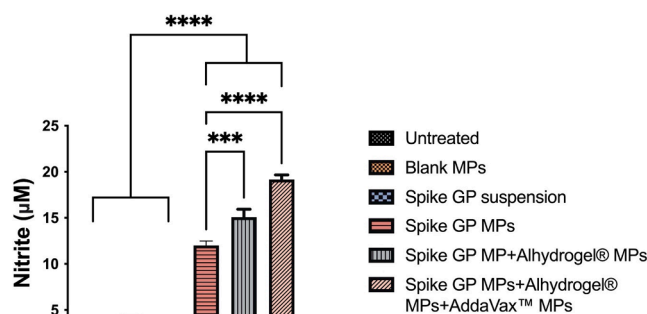


Fig. 4. Quantification of nitrite released by DC 2.4 upon 48 h of exposure to different treatment groups. Nitrite released by dendritic cells pulsed with spike GP MPs + Alhydrogel® MPs + AddaVax™ MPs was significantly higher as compared to spike suspension, spike GP MPs and spike GP + Alhydrogel® MPs. Data expressed as a mean ± SEM was analyzed using one-way ANOVA followed by post hoc Tukey's multiple comparison test. ***p < 0.001, ****p < 0.0001.

between multiple groups were analyzed using one-way Analysis of Variance (ANOVA) and two-way ANOVA followed by post-hoc analysis with Tukey's test. Data are expressed as mean ± SEM. For all the comparisons, a p-value < 0.05 was considered statistically significant. The following p values were used: ns-non-significant, (*)p < 0.05- significant, (**)p < 0.01-very significant, (***)p < 0.001-highly significant, (****)p < 0.0001-extremely significant.

3. Results

3.1. Formulation and characterization of MPs

The MPs were formulated using the double emulsion method and lyophilized. The percent recovery yield for the MPs was in the range of 88–91 %. The average particle size of spike GP MPs, Alhydrogel® MPs and AddaVax™ MPs was found to be 1.15 µm, 1.19 µm, and 1.05 µm respectively. The PDI for MPs was found to be in the range of 0.55–0.67. Zeta potential was found to be in the range of -20 mV to -25 mV (Table 2). The total protein content of Spike GP MPs was found to be 88.96 ± 7.58 %. The spike GP MPs and AddaVax™ MPs visualized using the SEM were found to be spherical. SEM images for Alhydrogel® MPs showed the MPs to be non-spherical (Fig. 3).

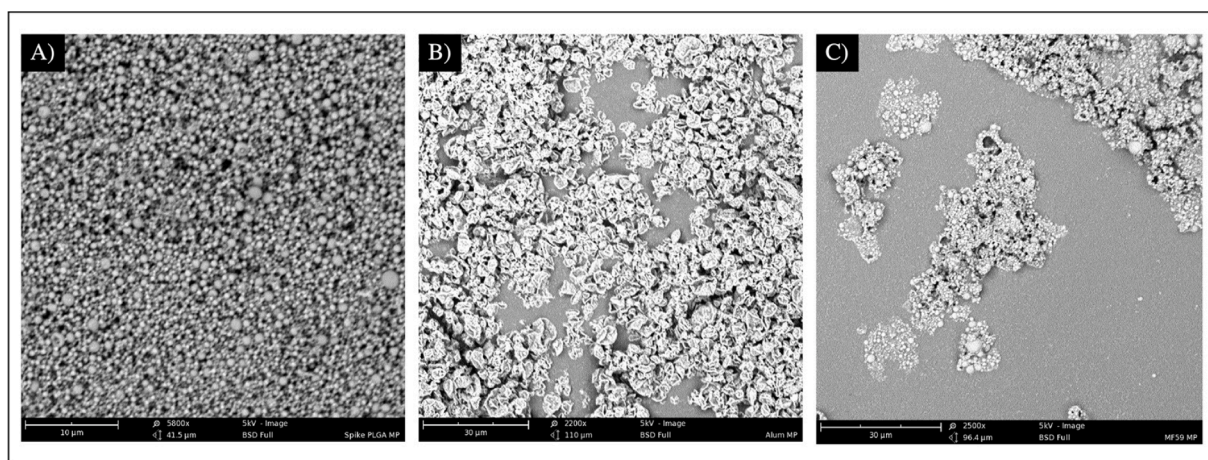


Fig. 3. SEM images representing morphology of Spike GP MPs, Alhydrogel® MP and Addavax™ MP from left to right. Scale bar. 10–30 µm.

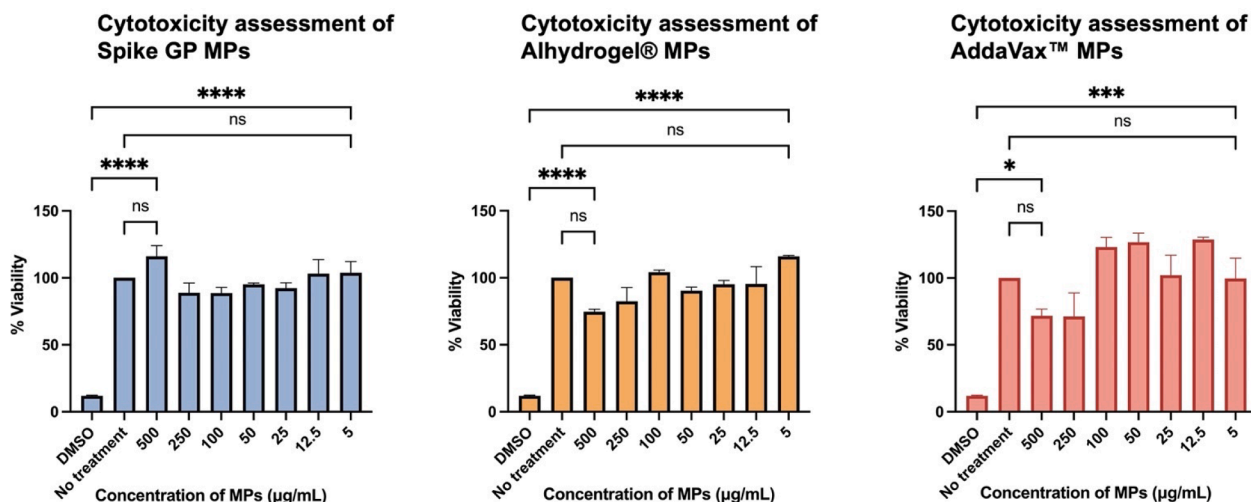


Fig. 5. Determination of cytotoxicity of MPs at increasing concentration. DC 2.4 were exposed to increasing amounts of vaccine antigen (Spike GP) or adjuvant (Alhydrogel® or Addavax™)-loaded microparticles and incubated for 24 h prior to being assessed for cytotoxicity of MPs. Data expressed as mean \pm SEM was analyzed using one-way ANOVA followed by post hoc Tukey's multiple comparison test. ns-not significant, ns-non significant, ****p < 0.0001.

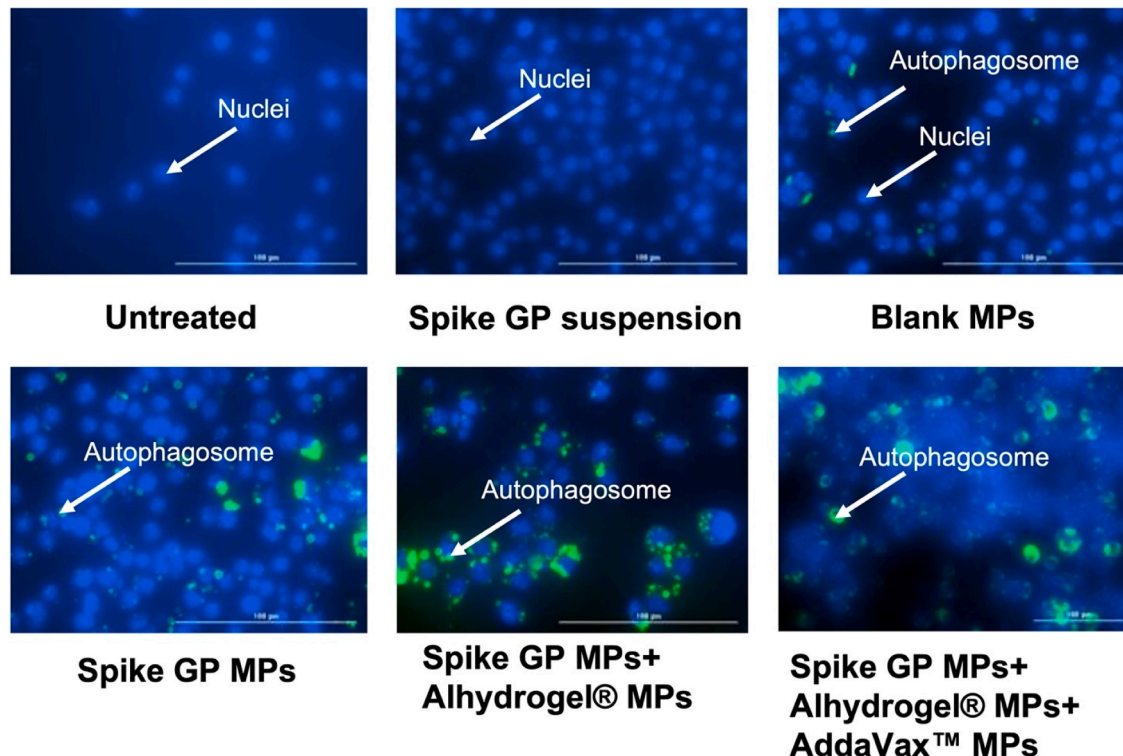


Fig. 6. Representative images showing expression of autophagosomes in dendritic cells. Dendritic cells were exposed to Spike GP Suspension, Blank MP, Spike GP MPs with and without adjuvants for 24 h. Dendritic cells were observed using fluorescence microscopy (20x) in a fluorescence microscope in which nuclei were stained with Hoechst 33,342 Nuclear stain (blue) and autophagosomes were stained with CYTO-ID® dye (green). (For interpretation of the references to color in this figure legend, the reader is referred to the web version of this article.)

3.2. Quantification of innate immune marker

Release of nitrite from the murine DC 2.4 in response to the different treatment groups was quantified using Griess's assay. We detected nitrite levels to be significantly higher in spike GP MP + Alhydrogel® MPs + AddaVax™ MPs and spike GP MPs + Alhydrogel® MPs groups as compared to spike GP suspension and spike GP MPs groups. DC 2.4 treated with blank MPs and untreated group did not produce significant nitrite levels (Fig. 4).

3.3. Assessment of cytotoxicity of MPs

DC 2.4 were exposed to increasing concentrations of Spike GP, Alhydrogel® or Addavax™ MPs ranging from 5 to 500 μ g per mL. We used an MTT assay to assess whether our MPs were toxic to DC 2.4. We observed that cells were at least 80 % viable for all particles at all concentrations tested. The percent cell viability was found to be inversely proportional to the concentration. At lower particle concentrations, the percent cell viability was higher than that of cells treated

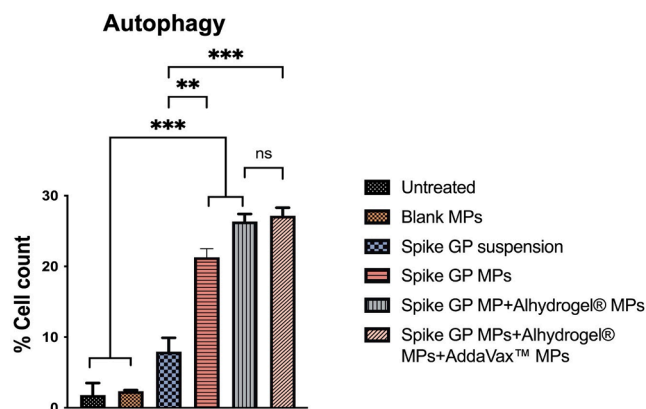


Fig. 7. Percent cell count of cells expressing autophagosomes when exposed to Spike GP MPs with and without adjuvants for 24 h. Data are expressed as mean \pm SEM analyzed using one-way ANOVA followed by post hoc Tukey's multiple comparison test. ** $p < 0.01$, *** $p < 0.001$.

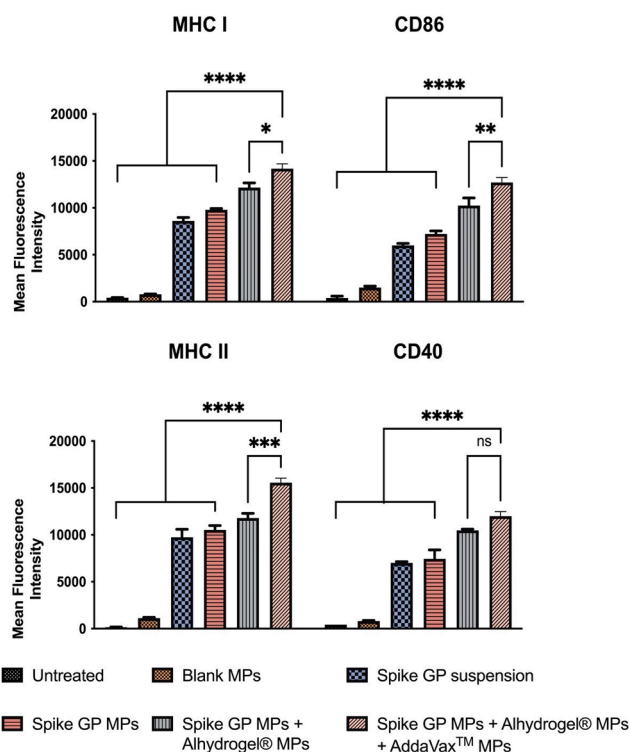


Fig. 8. Mean fluorescence intensity indicating expression of antigen-presenting molecules MHC I, its co-stimulatory molecule CD86 and MHC II and co-stimulatory molecule CD40 were analyzed using flow cytometry after staining with the respective markers. Dendritic cells were exposed for 48 h with the various treatment groups. Data expressed as mean \pm SEM was analyzed using one-way ANOVA followed by post-hoc analysis using Tukey's multiple comparison test. * $p < 0.05$, ** $p < 0.01$, *** $p < 0.001$, **** $p < 0.0001$.

with higher particle concentrations. Therefore, Spike GP MPs, Alhydrogel® MPs, and AddaVax™ MPs were non-cytotoxic to DC 2.4 cells (Fig. 5).

3.4. Assessment of the expression of autophagosomes in antigen presenting cells

DC 2.4 were exposed to different treatment groups and assessed for the expression of autophagosomes using fluorescence microscopy and flow cytometry. Fluorescence microscopic images revealed that DC 2.4

exposed with spike GP MPs, spike GP MPs + Alhydrogel® MPs, spike GP MPs + Alhydrogel® MPs + AddaVax™ MPs exhibited a higher number of autophagosomes compared to untreated, blank MPs, spike GP suspension groups. Similarly, when autophagosome expression was quantified using flow cytometry, it was observed that there was a higher percent of autophagosome expression in DC 2.4 exposed to spike GP MPs, spike GP MPs + Alhydrogel® MPs, spike GP MPs + Alhydrogel® MPs + AddaVax™ MPs as compared to untreated, Blank MPs, and Spike GP suspension groups (Figs. 6 and 7).

3.5. Quantification of expression of antigen presenting molecules MHC I, MHC II, and their co-stimulatory molecules CD86 and CD40

The expression of antigen-presenting molecules MHC I, MHC II, and their co-stimulatory molecules CD86, CD40 on DC 2.4 was assessed using flow cytometry. The MHC I and CD 86 levels expression in DC 2.4 exposed with spike GP MPs + Alhydrogel® MPs + AddaVax™ MPs was significantly higher compared to the spike GP suspension, spike GP MPs and spike GP MPs + Alhydrogel® MPs. Similarly, MHC II and CD 40 levels were also significantly high in the spike GP MPs + Alhydrogel® MPs + AddaVax™ MPs compared to the spike GP suspension, spike GP MPs and spike GP MPs + Alhydrogel® MPs (Fig. 8).

3.6. Formulation and characterization of dissolving MN vaccine

MPs-loaded dissolving MN were formulated using a spin-casting method. Formulated MN were observed to be uniform in shape and length as confirmed under SEM. Individual MN were measured for height, base width, and pitch length under SEM. MN height was about 506 μm , base width was 139 μm , and pitch was approximately 443 μm . The MN formed pores in the mouse skin and dissolved within 10 min as seen using SEM (Fig. 9).

3.7. Serum antibody responses in mice serum

We assessed the mice sera for the presence of IgM, IgG, IgG1 and IgG2a using ELISA. We observed that IgM levels peaked in mice vaccinated with spike GP MPs MN, (spike GP MPs + Alhydrogel® MPs) MN and (spike GP MPs + Alhydrogel® MPs + AddaVax™ MPs) MN at week 2 compared to the naïve group. IgM levels in the same group decreased after week 2 and remained insignificant until week 8. Total IgG levels in the sera were significantly high in spike GP MPs MN, (spike GP MPs + Alhydrogel® MPs) MN, (spike GP MPs + Alhydrogel® MPs + AddaVax™ MPs) MN as compared to naïve group at week 4 and remained significantly high until week 8. Total IgG levels were also significantly high in (spike GP MPs + Alhydrogel® MPs) MN as compared to the spike GP suspension MN group at week 4 and remained high until week 8. Mice vaccinated with (spike GP MPs + Alhydrogel® MPs + AddaVax™ MPs) MN showed significant total IgG levels compared to spike GP suspension MN at week 8, three weeks after second booster dose. We also observed that total IgG levels for mice that received (spike GP MPs + Alhydrogel® MPs + AddaVax™ MPs) MN at week 8 were significant compared to the same group total IgG levels at week 6. Total IgG levels after booster doses were also extremely significant for the same group compared to just one prime dose. Next, IgG1 levels were significantly higher in sera of mice vaccinated with (spike GP MPs + Alhydrogel® MPs) MN as compared to the naïve group at weeks 4, 6 and 8. We also observed that the IgG1 levels were very significant in (spike GP MPs + Alhydrogel® MPs) MN at week 8 after 3 doses compared to mice that received just the spike GP MPs MN. Data revealed that at week 8 (spike GP MPs + Alhydrogel® MPs + AddaVax™ MPs) MN showed significant levels of IgG1 compared to the naïve. Serum IgG1 levels in (spike GP MPs + Alhydrogel® MPs) MN were comparable to spike suspension MN group as the IgG1 as indicated by no significant difference in both the groups. Data also indicated that IgG2a levels were significantly higher in sera of mice who received (spike GP MPs + Alhydrogel® MPs +

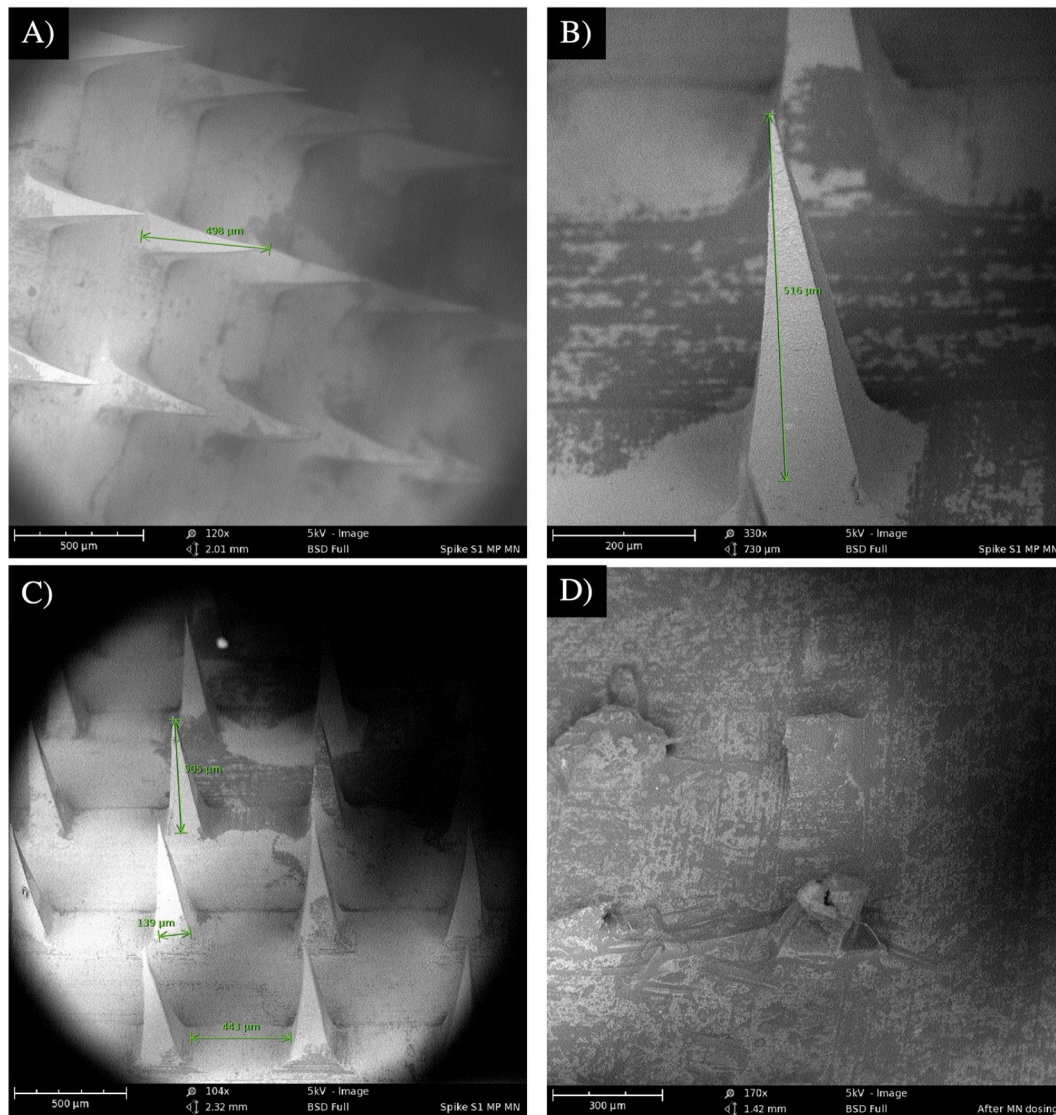


Fig. 9. SEM images representing (A) height of a microneedle in an array of microneedles (B) height of one microneedle (C) height, base length, and pitch length in a microneedle array (D) dissolved microneedles after vaccination to mice.

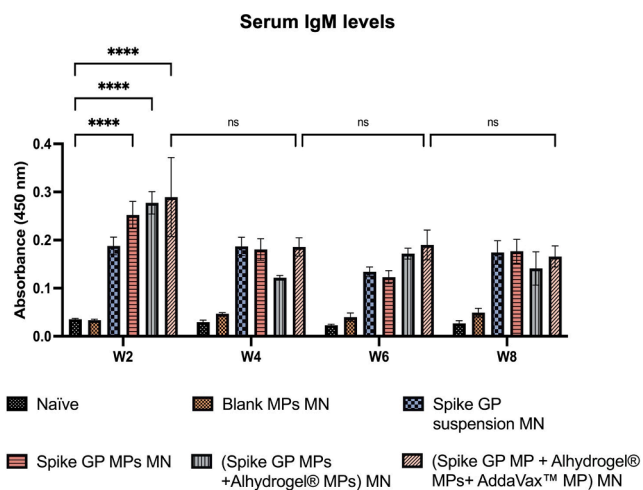


Fig. 10. Spike GP specific-antibody levels in serum for IgM measured after immunization of vaccinated and unvaccinated mice. The serum was analyzed using ELISA at a 1:50 dilution. Data are expressed as mean \pm SEM analyzed using two-way ANOVA followed by post-hoc analysis using Tukey's multiple comparison test-ns-not significant, ns-non significant, **** $p < 0.0001$.

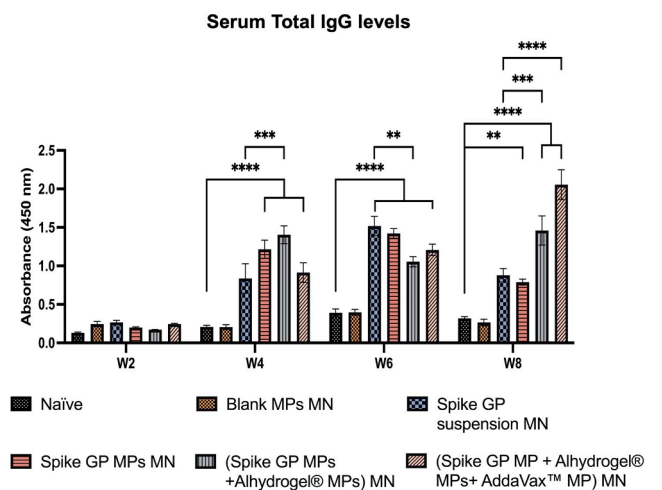


Fig. 11. Spike GP specific-antibody levels in serum for total IgG were measured in vaccinated and unvaccinated mice. Serum was analyzed using ELISA at dilution 1:50. Data are expressed as mean \pm SEM analyzed using two-way ANOVA followed by post hoc Tukey's multiple comparison test-** $p < 0.01$, *** $p < 0.001$, **** $p < 0.0001$.

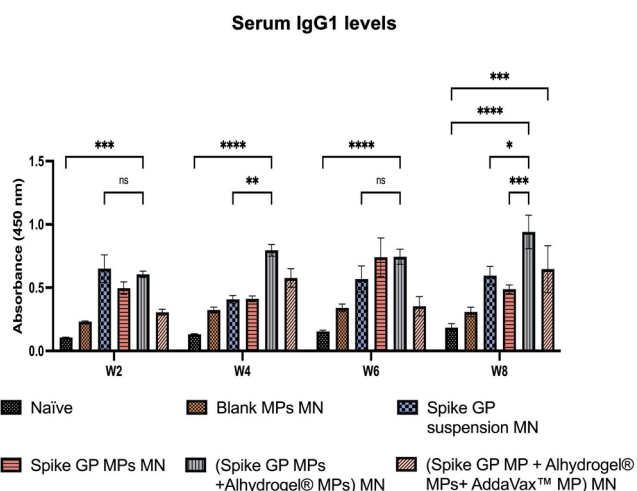


Fig. 12. Spike GP specific-antibody levels in serum for IgG1 measured in vaccinated and unvaccinated mice. Serum was analyzed using ELISA at dilution 1:50. Data are expressed as mean ± SEM analyzed using two-way ANOVA followed by post hoc Tukey’s multiple comparison test- ns- not significant, ns-non significant, *p < 0.05, **p < 0.01, ***p < 0.001, and ****p < 0.0001.

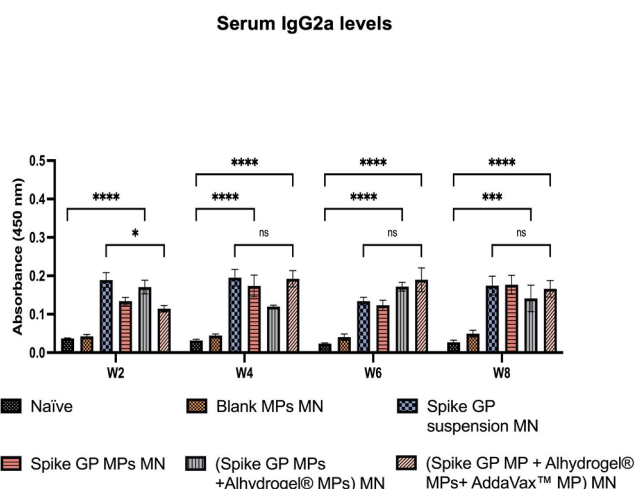


Fig. 13. Spike GP specific-antibody levels in serum for IgG2a measured in vaccinated and unvaccinated mice. Serum was analyzed using ELISA at dilution 1:50. Data are expressed as mean ± SEM analyzed using two-way ANOVA followed by post hoc Tukey’s multiple comparison test- ns- non significant, *p < 0.05, **p < 0.01, ***p < 0.001, and ****p < 0.0001.

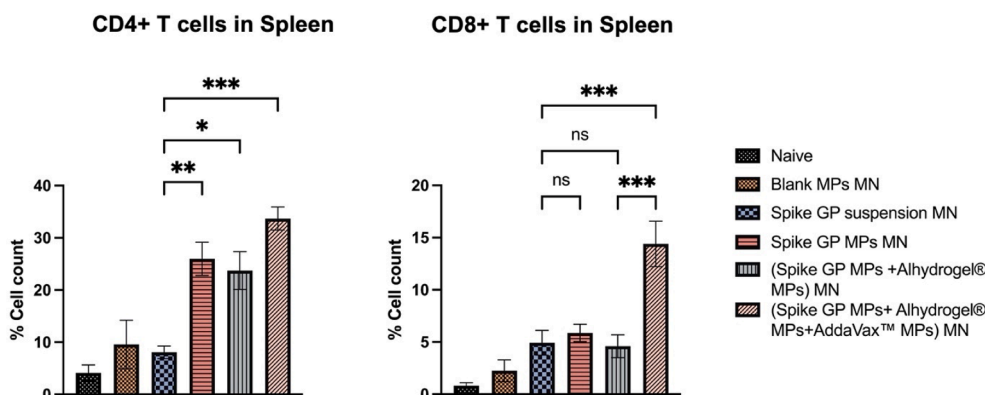


Fig. 14. CD4+ and CD8+ T cell responses in spleens of vaccinated and unvaccinated mice. Spleen samples were analyzed using flow cytometry. Data are expressed as mean ± SEM analyzed using one-way ANOVA followed by post hoc Tukey’s multiple comparison test- ns-non significant, *p < 0.05, **p < 0.01, ***p < 0.001, and ****p < 0.0001.

AddaVax™ MPs) MN as compared to naïve group at all weeks. We also observed that (spike GP MPs + Alhydrogel® MPs + AddaVax™ MPs) MN exhibited comparable levels of IgG2a in comparison with spike GP suspension MN group (Figs. 10–13).

3.8. Spike GP-specific T cell responses in spleen

Mice vaccinated with spike GP MPs MN, (spike GP MPs + Alhydrogel® MPs) MN and (spike GP MPs + Alhydrogel® MPs + AddaVax™ MPs) MN showed heightened expression CD4+ T cells as compared to the spike suspension group. (Spike GP MPs + Alhydrogel® MPs + AddaVax™ MPs) MN group also showed heightened expression of CD8+ T cells as compared to the (spike GP suspension) MN. Spike GP MPs MN (spike GP MPs + Alhydrogel® MPs) MN exhibited comparable CD8+ T cells compared to (spike GP suspension) MN group. CD4+ and CD8+ T cells in (spike GP MPs + Alhydrogel® MPs + AddaVax™ MPs) MN were significantly high as compared with (spike GP MPs + Alhydrogel® MPs) MN (Fig. 14).

4. Discussion

We demonstrated formulation, characterization and evaluated subunit vaccine such as spike GP encapsulated in PLGA polymer with and without adjuvant MPs *in vitro* in dendritic cells. We also demonstrated that an adjuvanted subunit vaccine encapsulated in polymeric MPs delivered using MN induces robust antibody-mediated and cellular responses against SARS-CoV in a preclinical murine model.

Polymeric MPs formulated using PLGA polymer is a multifaceted platform utilized in vaccine and therapeutic development. Polymeric MPs are beneficial as they offer protection to the antigen from degradation by enzymes and other extracellular agents (Menon et al., 2022). Especially, soluble recombinant protein as antigens such as spike GP with relatively less immunogenicity due to poor antigen cross-presentation (Storni et al., 2005). Thus, we formulated PLGA MPs encapsulating spike GP or adjuvants such as Alhydrogel® and AddaVax™. The particle size of spike GP MPs, Alhydrogel® MPs and AddaVax™ MPs were found to be in the range of 1.05–1.19 μm. Studies have shown that MPs of size 0.1–3 μm facilitate better acquisition and processing by APCs (Oyewumi et al., 2010). The protein content in the spike GP MPs was above 88 %; this indicated that our formulation method encapsulated most of the antigen. This promising result urged us to test the immunogenicity of these MPs *in vitro* in DC 2.4.

NO is one of the key players in controlling infectious diseases. It does so by activating APCs that enhances MHC-II expression and promotes chemotaxis by recruiting APCs. Apart from NO, its metabolites such as nitrite and nitrate are also involved in activating innate immune

response (Thwe and Amiel, 2018; Wink et al., 2011). Thus, we tested the production of nitrite in DC 2.4 in response to spike GP MPs with and without adjuvant MPs and in comparison, with spike GP suspension, blank MPs using Griess's assay. DC 2.4 exposed with MPs with and without adjuvant MPs produced significant amounts of nitrite as compared to spike GP suspension or blank MPs indicating that innate immune response was attributed to the antigen in the polymeric MPs and not just the polymeric MPs or antigen suspension.

Cell viability was assessed in APCs such as DC 2.4 which will interact closely with and process the antigen or adjuvant MPs to potentially elicit an immune response. More than 80 % of the cells were viable after treatment with spike GP MPs and adjuvant MPs in doses ranging from 5 to 500 µg/mL. Percent cell viability depends on the ability of metabolically active cells to convert MTT to purple formazan crystals (Principle and Protocol of MTT Assay (Cell Viability Assay), 2021). This data suggested that formulated PLGA MPs were non-cytotoxic to APCs and were thus used further for *in vitro* and *in vivo* immunogenicity assessment.

We also observed that adjuvanted spike GP MPs induced autophagosomes in DC 2.4 exposed with MPs compared to spike GP suspension or blank MPs. The size of the MPs likely also played a role in the upregulation of autophagosomes. Previous studies have shown enhanced uptake of MPs > 100 nm, which induces upregulation of autophagosomes (Menon et al., 2022). Our vaccine likely induced macro autophagy, which involves formation of a double membrane bound vesicle autophagosomes after phagocytosis of an exogenous antigen in MPs to the cytoplasm. Next, the MPs are degraded, the antigen is processed, and through a series of phagocytic events and antigen presentation presented as antigen-presenting molecules (MHC I, MHC II) and their co-stimulatory molecules (CD86, CD40) on the surface of the antigen-presenting cell. Past studies have shown that autophagy plays an important role in cross-presenting MHC I molecules on antigen-presenting cells (Klionsky et al., 2014; Puleston and Simon, 2014). We observed increased expression of MHC I, MHC II, CD86, and CD40 on dendritic cells which were exposed to spike GP MPs + Alhydrogel® MPs + AddaVax™ MPs as compared to spike GP suspension, spike GP MPs + Alhydrogel® MPs groups. These antigen presenting molecules and co-stimulatory molecules play a vital role in progressing the cellular immune response by presenting the antigen to T cell receptors and CD28 molecules which further leads to activation of CD8+ or CD4+ T cell (Kotsias et al., 2019; Zablon). Activated T cells can either induce a Th1 or Th2 immunity based on whether MHC I or MHC II pathway is used for antigen presentation (Blum et al., 2013). Apart from the various immunological advantages offered by MPs, we studied the intradermal vaccination route using dissolving MN for vaccine delivery. We tested this combined vaccination strategy *in vivo* for induction of humoral and cellular immunity to substantiate the enhanced *in vitro* immunogenicity by microparticulate vaccine.

Intradermal vaccination using dissolving MN delivering spike GP MPs with or without adjuvants as compared to MN delivering spike GP suspension has several advantages such as non-invasive route of administration and increased immunogenicity due to delivery of MPs to dermal layers that is rich with APCs (Sparber et al., 2010; Prausnitz et al., 2009). Studies utilizing MN vaccine delivery for proteins have proved to elicit robust vaccine efficacy in preclinical studies. The "PittCoVacc" vaccine, currently in development for phase I clinical trial, involves the administration of spike protein through dissolving MN (Kim et al., 2020; RePORTER).

Binding antibodies indicate the presence of a humoral response, which is vital in eliminating the virus by enhanced phagocytosis either by opsonization or complement-mediated lysis (Gunn and Alter, 2016). Thus, we evaluated the presence of antibody response in mice sera to MN delivering spike GP suspension, spike GP MPs and spike GP MPs with adjuvant MPs. Spike GP MPs with and without adjuvant MPs when delivered using MN also induced significant levels of IgM, IgG, and IgG subtypes after the prime dose in mice. Production of Spike GP-specific

IgM after the prime dose demonstrates the early antibody response after vaccination. Total IgG levels were significantly higher in mice vaccinated with spike GP MPs with and without adjuvant MPs compared to the spike GP suspension group after booster doses. This data suggested seroconversion of spike GP-specific IgM antibodies to spike GP-specific IgG antibodies in all the vaccinated mice as compared to the unvaccinated mice after booster doses.

Increase in the IgG1 levels indicates a Th2 skewed immune response whereas elevated IgG2a levels indicate Th1 skewed immune response. Thus, we further assessed the presence of IgG1 and IgG2a levels in vaccinated mice (Mountford et al., 1994; Woolard and Kumaraguru, 2010). Significant levels of Spike GP-specific IgG subtypes such as IgG1 and IgG2a indicated the presence of both Th1 and Th2 response essential for viral clearance. Mice vaccinated with (spike GP MPs + Alhydrogel® MPs) MN demonstrated high levels of IgG1 indicating an Alhydrogel® biased Th2 immune response. Further, IgG1 and IgG2a levels in spike GP MPs + Alhydrogel® MPs + AddaVax™ MPs group indicated that AddaVax™ promoted both Th1 and Th2 immune response. Our adjuvanted microparticulate vaccine produced significant levels of antibodies compared to Blank MP MN group, thus indicating that the response was antigen-specific and not directed towards the microparticulate or MN matrix. The presence of binding antibodies indicates that the vaccine MPs were able to elicit spike GP-specific IgM, IgG, and IgG subtypes antibody-mediated responses. In future studies, we will explore the neutralizing capacity of the Spike GP-induced antibodies elicited by our spike GP MPs delivered by MN by evaluating the levels of Spike GP-specific neutralizing antibodies.

When APCs present the antigen via the MHC-II pathway helper T cells are activated, representing a Th2 type of immune response. Moreover, activation of cytotoxic T lymphocytes (CTL) occurs when APCs present antigen via the MHC-I pathway indicating Th1 type immune response. The presence of CTL is vital in vaccines against viral infections causing the execution of virus-infected cells. Thus, we studied the presence of both spike GP-specific CD4+ T cells and CD8+ T cells in the spleen. We found that mice vaccinated with spike GP MPs + Alhydrogel® MPs + AddaVax™ MPs induced significant levels of helper T cells and cytotoxic T cells compared to the spike GP suspension. This further validated the presence of Th1 and Th2 immune responses in mice vaccinated with (spike GP MPs + Alhydrogel® MPs + AddaVax™ MPs) MN.

Thus, in this proof-of-concept study we demonstrate that dissolving MN used to deliver MPs encapsulating spike GP as a subunit antigen is an efficient vaccine delivery strategy against coronaviruses. However, spike GP of the SARS-CoV virus is a model antigen, and further studies with spike SARS-CoV-2 antigen will aid in developing a non-invasive vaccination strategy against the ongoing COVID-19 pandemic. Thus, we are currently investigating the SARS-CoV-2 spike receptor binding domain as a more suitable antigen candidate.

5. Conclusion

This proof-of-concept study established that MN used to deliver a subunit antigen candidate like spike GP in microparticulate form along with adjuvant MPs intradermally showed enhanced humoral and cellular responses *in vivo*. *In vitro* testing indicated that spike GP MPs and adjuvant MPs heightened innate immunity and were readily taken up by APCs, showing enhanced production of autophagosomes, which correlated to the increased expression of antigen-presenting molecules. The spike GP/adjuvant MPs vaccine was shown to be non-cytotoxic towards APCs. Thus, Spike GP MP + adjuvant MPs loaded in dissolving micro-needles is an efficacious vaccine candidate against SARS-CoV, which can aid in developing a future pain-free vaccination against COVID-19.

Funding

This study did not receive funding from any grants in either public,

commercial, or non-profit sectors.

CRediT authorship contribution statement

Smital Patil: Conceptualization, Investigation, Methodology, Data curation, Formal analysis, Validation, Visualization, Writing - original draft, Writing - review & editing. **Sharon Vijayanand:** Conceptualization, Methodology, Writing - review & editing. **Devyani Joshi:** Formal analysis, Methodology, Writing - review & editing. **Ipshita Menon:** Methodology, Writing - review & editing. **Keegan Braz Gomes:** Methodology, Writing - review & editing. **Akanksha Kale:** Methodology, Writing - review & editing. **Priyar Bagwe:** Methodology, Writing - review & editing. **Shadi Yacoub:** Methodology. **Mohammad N. Uddin:** Writing - review & editing. **Martin J. D'Souza:** Conceptualization, Funding acquisition, Supervision, Project administration, Writing - review & editing.

Declaration of Competing Interest

The authors declare that they have no known competing financial interests or personal relationships that could have appeared to influence the work reported in this paper.

Data availability

Data will be made available on request.

Acknowledgment

“The following reagent was obtained through BEI Resources, NIAID, NIH: SARS-CoV Spike (S) Protein delta™, Recombinant from Baculovirus, NR-722.”

Graphical abstract and other figures created with [Biorender.com](https://www.biorender.com).

References

- AddVax™. InvivoGen. <https://www.invivogen.com/addavax> (accessed 2022-07-12).
- Allahyari, M., Mohit, E., 2015. Peptide/protein vaccine delivery system based on PLGA particles. *Hum. Vaccines Immunother.* 12 (3), 806–828. <https://doi.org/10.1080/21645515.2015.1102804>.
- Bilati, U., Allémann, E., Doelker, E., 2005. Strategic approaches for overcoming peptide and protein instability within biodegradable nano- and microparticles. *Eur. J. Pharm. Biopharm.* 59 (3), 375–388. <https://doi.org/10.1016/j.ejpb.2004.10.006>.
- Blum, J.S., Wearsch, P.A., Cresswell, P., 2013. Pathways of antigen processing. *Annu. Rev. Immunol.* 31, 443–473. <https://doi.org/10.1146/annurev-immunol-032712-095910>.
- Braz Gomes, K., D'Souza, B., Vijayanand, S., Menon, I., D'Souza, M.J., 2022. A dual-delivery platform for vaccination using antigen-loaded nanoparticles in dissolving microneedles. *Int. J. Pharm.* 613, 121393. <https://doi.org/10.1016/j.ijpharm.2021.121393>.
- Brewer, J.M., 2006. (How) do aluminium adjuvants work? *Immunol. Lett.* 102 (1), 10–15. <https://doi.org/10.1016/j.imlet.2005.08.002>.
- Carcaboso, A.M., Hernández, R.M., Igartua, M., Rosas, J.E., Patarroyo, M.E., Pedraz, J.L., 2004. Enhancing immunogenicity and reducing dose of microparticulated synthetic vaccines: single intradermal administration. *Pharm. Res.* 21 (1), 121–126. <https://doi.org/10.1023/b:pham.0000012159.20895.5b>.
- Du, L., He, Y., Zhou, Y., Liu, S., Zheng, B.-J., Jiang, S., 2009. The spike protein of SARS-CoV — a target for vaccine and therapeutic development. *Nat. Rev. Microbiol.* 7 (3), 226–236. <https://doi.org/10.1038/nrmicro2090>.
- Full article: Advances in aluminum hydroxide-based adjuvant research and its mechanism. <https://www.tandfonline.com/doi/full/10.1080/21645515.2014.1004026> (accessed 2022-08-09).
- Gala, R.P., Zaman, R.U., D'Souza, M.J., Zughair, S.M., 2018. Novel whole-cell inactivated *Neisseria gonorrhoeae* microparticles as vaccine formulation in microneedle-based transdermal immunization. *Vaccines* 6 (3), 60. <https://doi.org/10.3390/vaccines6030060>.
- Giordano, D., De Masi, L., Argenio, M.A., Facchiano, A., 2021. Structural dissection of viral spike-protein binding of SARS-CoV-2 and SARS-CoV-1 to the human angiotensin-converting enzyme 2 (ACE2) as cellular receptor. *Biomedicines* 9 (8), 1038. <https://doi.org/10.3390/biomedicines9081038>.
- Gunn, B.M., Alter, G., 2016. Modulating antibody functionality in infectious disease and vaccination. *Trends Mol. Med.* 22 (11), 969–982. <https://doi.org/10.1016/j.molmed.2016.09.002>.
- Hatmal, M.M., Alshaer, W., Al-Hatamleh, M.A.I., Hatmal, M., Smadi, O., Taha, M.O., Oweida, A.J., Boer, J.C., Mohamud, R., Plebanski, M., 2020. Comprehensive

- structural and molecular comparison of spike proteins of SARS-CoV-2, SARS-CoV and MERS-CoV, and their interactions with ACE2. *Cells* 9 (12), 2638. <https://doi.org/10.3390/cells9122638>.
- Alhydrogel | Alum vaccine adjuvant for research | InvivoGen. <https://www.invivogen.com/alhydrogel> (accessed 2022-07-12).
- Joshi, D., Gala, R.P., Uddin, M.N., D'Souza, M.J., 2021. Novel ablative laser mediated transdermal immunization for microparticulate measles vaccine. *Int. J. Pharm.* 606, 120882. <https://doi.org/10.1016/j.ijpharm.2021.120882>.
- Joshi, D., Chbib, C., Uddin, M.N., D'Souza, M.J., 2021. Evaluation of microparticulate (S)-4,5-dihydroxy-2,3-pentanedione (DPD) as a potential vaccine adjuvant. *AAPS J.* 23 (4), 84. <https://doi.org/10.1208/s12248-021-00617-6>.
- Kim, E., Erdos, G., Huang, S., Kenniston, T.W., Balmert, S.C., Carey, C.D., Raj, V.S., Epperly, M.W., Klimstra, W.B., Haagmans, B.L., Korkmaz, E., Falo, L.D., Gambotto, A., 2020. Microneedle array delivered recombinant coronavirus vaccines. Immunogenicity and rapid translational development. *EBioMedicine* 55, 102743. <https://doi.org/10.1016/j.ebiom.2020.102743>.
- Klionsky, D.J., Eskelinen, E.-L., Deretic, V., 2014. Autophagosomes, phagosomes, autolysosomes, phagolysosomes, autophagolysosomes... wait, I'm confused. *Autophagy* 10 (4), 549–551. <https://doi.org/10.4161/aut.28448>.
- Kotsias, F., Cebrian, I., Alloati, A., 2019. Antigen processing and presentation. *Int. Rev. Cell Mol. Biol.* 348, 69–121. <https://doi.org/10.1016/bs.ircmb.2019.07.005>.
- Leleux, J., Roy, K., 2013. Micro and nanoparticle-based delivery systems for vaccine immunotherapy: an immunological and materials perspective. *Adv. Healthc. Mater.* 2 (1), 72–94. <https://doi.org/10.1002/adhm.201200268>.
- Leone, M., Mönkäre, J., Bouwstra, J.A., Kersten, G., 2017. Dissolving microneedle patches for dermal vaccination. *Pharm. Res.* 34 (11), 2223–2240. <https://doi.org/10.1007/s11095-017-2223-2>.
- Ma, C., Su, S., Wang, J., Wei, L., Du, L., Jiang, S., 2020. From SARS-CoV to SARS-CoV-2: safety and broad-spectrum are important for coronavirus vaccine development. *Microbes Infect.* 22 (6), 245–253. <https://doi.org/10.1016/j.micinf.2020.05.004>.
- Menon, I., Bagwe, P., Gomes, K.B., Bajaj, L., Gala, R., Uddin, M.N., D'Souza, M.J., Zughair, S.M., 2021. Microneedles: a new generation vaccine delivery system. *Micromachines* 12 (4), 435. <https://doi.org/10.3390/mi12040435>.
- Menon, I., Kang, S.M., D'Souza, M., 2022. Nanoparticle formulation of the fusion protein virus like particles of respiratory syncytial virus stimulates enhanced in vitro antigen presentation and autophagy. *Int. J. Pharm.* 623, 121919. <https://doi.org/10.1016/j.ijpharm.2022.121919>.
- Middle East respiratory syndrome coronavirus (MERS-CoV). <https://www.who.int/h-health-topics/middle-east-respiratory-syndrome-coronavirus-mers> (accessed 2022-08-07).
- Mountford, A.P., Fisher, A., Wilson, R.A., 1994. The profile of IgG1 and IgG2a antibody responses in mice exposed to *Schistosoma Mansoni*. *Parasite Immunol.* 16 (10), 521–527. <https://doi.org/10.1111/j.1365-3024.1994.tb00306.x>.
- Munro, A.P.S., Feng, S., Janani, L., Cornelius, V., Aley, P.K., Babbage, G., Baxter, D., Bula, M., Cathie, K., Chatterjee, K., Dodd, K., Enever, Y., Qureshi, E., Goodman, A.L., Green, C.A., Harndahl, L., Haughney, J., Hicks, A., van der Klauuw, A.A., Kanji, N., Libri, V., Llewelyn, M.J., McGregor, A.C., Maallah, M., Minassian, A.M., Moore, P., Mughal, M., Mujadidi, Y.F., Holliday, K., Osanlou, O., Osanlou, R., Owens, D.R., Pacurar, M., Palfreeman, A., Pan, D., Rampling, T., Regan, K., Saich, S., Bawa, T., Saralaya, D., Sharma, S., Sheridan, R., Thomson, E.C., Todd, S., Twelves, C., Read, R. C., Charlton, S., Hallis, B., Ramsay, M., Andrews, N., Lambe, T., Nguyen-Van-Tam, J. S., Snape, M.D., Liu, X., Faust, S.N., 2022. Safety, immunogenicity, and reactivity of BNT162b2 and mRNA-1273 COVID-19 vaccines given as fourth-dose boosters following two doses of ChAdOx1 NCoV-19 or BNT162b2 and a third dose of BNT162b2 (COV-BOOST): a multicentre, blinded, phase 2, randomised trial. *Lancet Infect. Dis.* 22 (8), 1131–1141. [https://doi.org/10.1016/S1473-3099\(22\)00271-7](https://doi.org/10.1016/S1473-3099(22)00271-7).
- O'Hagan, D.T., Singh, M., 2003. Microparticles as vaccine adjuvants and delivery systems. *Expert Rev. Vaccines* 2 (2), 269–283. <https://doi.org/10.1586/14760584.2.2.269>.
- Oyewumi, M.O., Kumar, A., Cui, Z., 2010. Nano-microparticles as immune adjuvants: correlating particle sizes and the resultant immune responses. *Expert Rev. Vaccines* 9 (9), 1095–1107. <https://doi.org/10.1586/erv.10.89>.
- Nano-Microparticle Platforms in Developing Next-Generation Vaccines - PMC. <http://www.ncbi.nlm.nih.gov/pmc/articles/PMC8228777/> (accessed 2022-08-09).
- Prausnitz, M.R., Mikszta, J.A., Cormier, M., Andrianov, A.K., 2009. Microneedle-based vaccines. *Curr. Top. Microbiol. Immunol.* 333, 369–393. https://doi.org/10.1007/978-3-540-92165-3_18.
- Principle and protocol of MTT assay (cell viability assay), 2021. <https://www.youtube.com/watch?v=Dn5WgYd0vpU> (accessed 2022-04-04).
- Pulendran, B., Arunachalam, S.P., O'Hagan, D.T., 2021. Emerging concepts in the science of vaccine adjuvants. *Nat. Rev. Drug Discov.* 20(6), 454–475. doi: 10.1038/s41573-021-00163-y.
- Puleston, D.J., Simon, A.K., 2014. Autophagy in the immune system. *Immunology* 141 (1), 1–8. <https://doi.org/10.1111/imm.12165>.
- RePORT | RePORTER. <https://reporter.nih.gov/search/zLkEsG2LhUKQWqvXy4rTtg/project-details/10147381> (accessed 2022-07-12).
- Rice-Ficht, A.C., Arenas-Gamboa, A.M., Kahl-McDonagh, M.M., Ficht, T.A., 2010. Polymeric particles in vaccine delivery. *Curr. Opin. Microbiol.* 13 (1), 106–112. <https://doi.org/10.1016/j.mib.2009.12.001>.
- Ritchie, H., Mathieu, E., Rodés-Guirao, L., Appel, C., Giattino, C., Ortiz-Ospina, E., Hasell, J., Macdonald, B., Beltekian, D., Roser, M., 2020. Coronavirus Pandemic (COVID-19). Our World Data.
- Silva, A.L., Soema, P.C., Slütter, B., Ossendorp, F., Jiskoot, W., 2016. PLGA particulate delivery systems for subunit vaccines: linking particle properties to immunogenicity.

- Hum. Vaccines Immunother. 12 (4), 1056–1069. <https://doi.org/10.1080/21645515.2015.1117714>.
- Smith, T.R.F., Patel, A., Ramos, S., Elwood, D., Zhu, X., Yan, J., Gary, E.N., Walker, S.N., Schultheis, K., Purwar, M., Xu, Z., Walters, J., Bhojnarwala, P., Yang, M., Chokkalingam, N., Pezzoli, P., Parzych, E., Reuschel, E.L., Doan, A., Tursi, N., Vasquez, M., Choi, J., Tello-Ruiz, E., Maricic, I., Bah, M.A., Wu, Y., Amante, D., Park, D.H., Dia, Y., Ali, A.R., Zaidi, F.I., Generotti, A., Kim, K.Y., Herring, T.A., Reeder, S., Andrade, V.M., Buttigieg, K., Zhao, G., Wu, J.-M., Li, D., Bao, L., Liu, J., Deng, W., Qin, C., Brown, A.S., Khoshnejad, M., Wang, N., Chu, J., Wrapp, D., McLellan, J.S., Muthumani, K., Wang, B., Carroll, M.W., Kim, J.J., Boyer, J., Kulp, D. W., Humeau, L.M.P.F., Weiner, D.B., Broderick, K.E., 2020. Immunogenicity of a DNA vaccine candidate for COVID-19. *Nat. Commun.* 11, 2601. <https://doi.org/10.1038/s41467-020-16505-0>.
- Sparber, F., Tripp, C.H., Hermann, M., Romani, N., Stoitzner, P., 2010. Langerhans cells and dermal dendritic cells capture protein antigens in the skin: possible targets for vaccination through the skin. *Immunobiology* 215 (9–10), 770–779. <https://doi.org/10.1016/j.imbio.2010.05.014>.
- Storni, T., Kündig, T.M., Senti, G., Johansen, P., 2005. Immunity in response to particulate antigen-delivery systems. *Adv. Drug Deliv. Rev.* 57 (3), 333–355. <https://doi.org/10.1016/j.addr.2004.09.008>.
- Streilein, J.W., 1983. Skin-associated lymphoid tissues (SALT): origins and functions. *J. Invest. Dermatol.*; 0022202X, 80, 12s–16s. doi: 10.1038/jid.1983.4.
- Thwe, P.M., Amiel, E., 2018. The role of nitric oxide in metabolic regulation of dendritic cell immune function. *Cancer Lett.* 412, 236–242. <https://doi.org/10.1016/j.canlet.2017.10.032>.
- Wink, D.A., Hines, H.B., Cheng, R.Y.S., Switzer, C.H., Flores-Santana, W., Vitek, M.P., Ridnour, L.A., Colton, C.A., 2011. Nitric oxide and redox mechanisms in the immune response. *J. Leukoc. Biol.* 89 (6), 873–891. <https://doi.org/10.1189/jlb.1010550>.
- Woolard, S.N., Kumaraguru, U., 2010. Viral vaccines and CTL response. *J. Biomed. Biotechnol.* 2010, 141657 <https://doi.org/10.1155/2010/141657>.
- Zablón, F.M. MHC Molecules, Antigen Processing and Presentation. *The Biology Notes*. <https://thebiologynotes.com/mhc-molecules-antigen-processing-presentation/> (accessed 2021-09-13).